GPS Precise Point Positioning
Using IGS Orbit Products

Jan Kouba and Pierre Héroux
Geodetic Survey Division
Natural Resources Canada
615 Booth Street
Ottawa, Ontario
K1A 0E9

September 2000

Abstract

The International GPS Service (IGS) has provided GPS orbit products to the scientific community with increased precision and timeliness. Many users interested in geodetic positioning have adopted the IGS precise orbits to achieve centimeter level accuracy and ensure long-term reference frame stability. Currently, a differential positioning approach that requires the combination of observations from a minimum of two GPS receivers, with at least one occupying a station with known coordinates is commonly used. The user position can then be estimated relative to one or multiple reference stations using differenced carrier phase observations and a baseline or network estimation approach. Differencing observations is a popular way to cancel out common GPS satellite and receiver clock errors. Baseline or network processing is effective in connecting the user position to the coordinates of the reference stations while the precise orbit virtually eliminates the errors introduced by the GPS space segment. This mode of processing has proven to be very effective and has received widespread acceptance. One drawback is the practical constraint imposed by the requirement that simultaneous observations be made at reference stations.

The following details a post-processing approach that uses un-differenced dual-frequency pseudorange and carrier phase observations along with IGS precise orbit products, for stand-alone precise geodetic point positioning (static or kinematic) with centimeter precision. This is possible if one takes advantage of the satellite clock estimates available with the satellite coordinates in the IGS precise orbit products and models systematic effects that cause centimeter variations in the satellite to user range. This paper will describe the approach, summarize the adjustment procedure and specify the earth and space based models that must be implemented to achieve centimeter level positioning in static mode. Furthermore, station tropospheric zenith path delays with centimetre precision and GPS receiver clock estimates precise to 0.1 nanosecond are also obtained.

Introduction

The Geodetic Survey Division (GSD) of Natural Resources Canada (NRCan), formerly Energy, Mines and Resources (EMR), has been an active participant in the International GPS Service since its pilot phase in 1992. As one of seven IGS Analysis Centers known as EMR, GSD contributes daily predicted, rapid and final GPS orbits and clocks to the IGS combinations. Recently, an ultra-rapid product to serve meteorological applications and support Low Earth Orbiter (LEO) missions has been added to the GSD's product submissions to the IGS. GSD has also played a key role in the past as the IGS Analysis Center (AC) Coordination Center and is now responsible for IGS Reference Frame Coordination, contributing together with other space techniques to the International Earth Rotation Service (IERS) realization of the International Terrestrial Reference Frame (ITRF). The daily computation of global precise GPS orbits and clocks is one way the GSD has chosen to support the Canadian Spatial Reference System (CSRS) in order to connect it into the ITRF and facilitate the integration of GPS surveys within Canada. The daily

availability of data from a number of tracking stations that are part of the Canadian Active Control System (CACS) along with precise GPS orbit products provide Canadian GPS users the opportunity to link directly into the CSRS and position themselves within a globally integrated reference frame (ITRF) with centimeter accuracy.

For GPS users interested in meter level positioning, a simple point positioning interface combining pseudorange data with precise orbits and clocks can be used. GSD uses 30-second tracking data from selected IGS stations with stable atomic clocks (Héroux and Kouba, 1995) and precise IGS satellite clocks at 15 minute intervals to produce 30-second precise satellite clocks. These products satisfy GPS users observing at high data rates in either static or kinematic modes for applications requiring meter precision. For GPS users seeking to achieve geodetic precision, sophisticated processing software such as GIPSY (Lichten et al., 1995), BERNESE (Rothacher and Mervart, 1996) and GAMIT (King and Bock, 1999) are required. By using the IGS precise orbit products and combining the GPS carrier phase data with CACS observations, geodetic users achieve precise positioning while integrating into the CSRS. Software provided by receiver manufacturers may also be used as long as it allows for the input of station and orbit data in standard format.

Recently, precise point positioning (PPP) algorithms using un-differenced carrier phase observations have been added to software suites such as GIPSY and the traditional double-differencing BERNESE. Users now have the option of processing data from a single station to obtain positions with centimeter precision within the reference frame provided by the IGS orbit products. NRCan PPP software also evolved from its original version (Héroux et al., 1993) to provide increasing precision. Point positioning eliminates the need to acquire simultaneous tracking data from a reference (base) station or a network of stations. It has given rise to centralized geodetic positioning services that require from the user the simple submission of a request and valid GPS observation file (see e.g. Zumberge, 1999). The approach presented here is an implementation of precise point positioning that effectively distributes processing by providing portable software that can be used on a personal computer and takes advantage of the highly accurate global reference frame made available through the IGS orbit products.

The IGS GPS Orbit Products

The IGS Precise Orbit products come in various flavors, from the Final, Rapid and Predicted to the unofficial Ultra-Rapid. They differ mainly by their varying latency and the extent of the tracking network used for their computation. The IGS Final orbits are combined from up to 7 contributing IGS Analysis Centers (ACs) and are usually available on the eleventh day after the last observation. The Rapid orbit product is combined 17 hours after the end of the day of interest. The latency is mainly due to the varying availability of tracking data from stations of the global IGS tracking network, which use a variety of data acquisition and communication schemes. In the past, the IGS products have been based on a daily model that required submissions of files containing tracking data for 24-hour periods. Recently, Data Centers have been asked to forward hourly tracking data to accelerate product delivery. This new submission scheme was required for the creation of an Ultra-Rapid product, with a latency of only a few hours, that should satisfy the more demanding needs of the meteorological community and future LEO (Low Earth Orbiter) missions. It is expected that IGS products will continue to be delivered with increased timeliness in the future (Neilan et al., 1997, Kouba et al., 1998).

Regarding the IGS orbit precision, one can see that over the past 8 years (Figure 1), the quality of the IGS Final orbits has improved from about 30 cm to the 3-5 cm precision level currently realized by some of the AC's (Kouba, 1998 IGS Annual Report). It is also interesting to note that the Rapid orbit combined product is as precise as the best AC Final solution with less tracking stations and faster delivery time. This fact confirms the belief that increasing the number of global GPS tracking stations does not necessarily translate into higher orbit precision. One element that has not yet received much attention is the quality of the GPS satellite clock estimates included in the IGS orbit products. Examining the IGS Final summary reports (http://igscb.jpl.nasa.gov/mail/igsreports/) produced weekly by the IGS AC coordinator (Dr. T. Springer, Astronomical Institute, University of Berne), we notice that satellite clock estimates produced by

different AC's agree within 0.1-0.2 nanosecond RMS, or 3-6 cm, a level which is compatible with the orbit precision. The combination of precise GPS orbits and clocks, weighted according to their corresponding sigmas, is essential for PPP, given that the proper measurements are made at the user set and the observation models are correctly implemented.

Figure 1: Weighted Orbit RMS of the IGS Rapid and AC Final orbit solutions with Respect to the IGS Final Orbit Products (1998 IGS Annual Report, IGS Central Bureau)

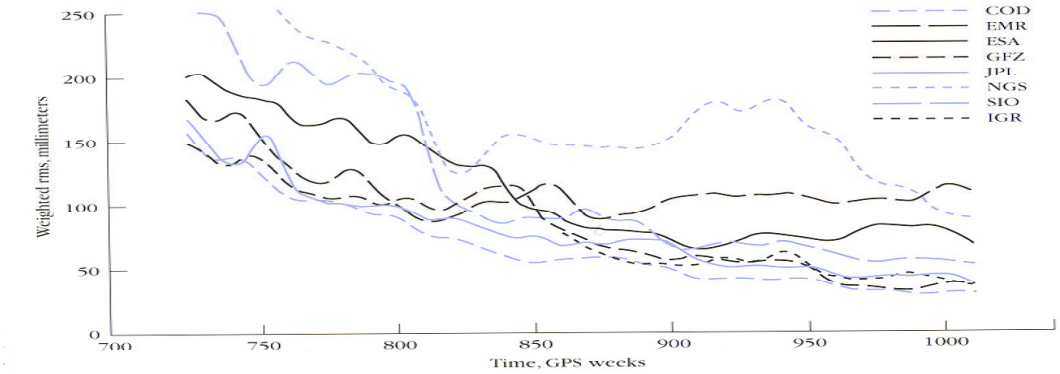

Precise Point Positioning

Observation Equations

The ionospheric-free combinations of dual-frequency GPS pseudorange (P) and carrier-phase observations (Φ) are related to user position, clock, troposphere and ambiguity parameters according to the following simplified observation equations:

$$\ell_P = \rho + C(dt\text{-}dT) + T_r + \varepsilon_P \quad (1)$$

$$\ell_\Phi = \rho + C(dt\text{-}dT) + T_r + N\lambda + \varepsilon_\Phi \quad (2)$$

where:

ℓ_P	is the ionosphere-free combination of L1 and L2 pseudoranges ($2.54P_1$-$1.54P_2$),
ℓ_Φ	is the ionosphere-free combination of L1 and L2 carrier-phases ($2.54\phi_1$-$1.54\phi_2$),
dt	is the station clock offset from GPS time,
dT	is the satellite clock offset from GPS time,
C	is the vacuum speed of light,
T_r	is the signal path delay due to the neutral-atmosphere (primarily the troposphere),
λ	is the carrier, or carrier-combination, wavelength,
N	is the ambiguity of the carrier-phase ionosphere-free combination, and
ε_P, ε_Φ	are the relevant measurement noise components, including multipath.

Symbol ρ is the geometrical range computed as a function of satellite (Xs, Ys, Zs) and station (x, y, z) coordinates according to:

$$\rho = \sqrt{(Xs-x)^2 + (Ys-y)^2 + (Zs-z)^2} \quad .$$

Expressing the tropospheric path delay (T_r) as a function of the zenith path delay (*zpd*) and mapping function (*M*) and removing the known satellite clocks (*dT*) gives the following mathematical model in the simplest form:

$$f_P = \rho + C\,dt + M\,zpd + \varepsilon_P - \ell_P = 0 \quad (3)$$

$$f_\Phi = \rho + C\,dt + M\,zpd + N\,\lambda + \varepsilon_\Phi - \ell_\Phi = 0 \quad (4)$$

Adjustment Model

Linearization of observation equations (3) and (4) around the a-priori parameters and observations (X^0, ℓ) becomes, in matrix form:

$$A\,\delta + W - V = 0,$$

where *A* is the design matrix, δ is the vector of corrections to the unknown parameters *X*, $W = f(X^0, \ell)$ is the misclosure vector and *V* is the vector of residuals.

The partial derivatives of the observation equations with respect to *X*, consisting of four types of parameters: station position (*x*,*y*,*z*), clock (*dt*), troposphere zenith path delay (*zpd*) and (non-integer) carrier-phase ambiguities (*N*), form the design matrix *A*:

$$A = \begin{bmatrix} \frac{\partial f(X,\ell_P)}{\partial X_x} & \frac{\partial f(X,\ell_P)}{\partial X_y} & \frac{\partial f(X,\ell_P)}{\partial X_z} & \frac{\partial f(X,\ell_P)}{\partial X_{dt}} & \frac{\partial f(X,\ell_P)}{\partial X_{zpd}} & \frac{\partial f(X,\ell_P)}{\partial X_{N^j_{(j=1,nsat)}}} \\ \frac{\partial f(X,\ell_\Phi)}{\partial X_x} & \frac{\partial f(X,\ell_\Phi)}{\partial X_y} & \frac{\partial f(X,\ell_\Phi)}{\partial X_z} & \frac{\partial f(X,\ell_\Phi)}{\partial X_{dt}} & \frac{\partial f(X,\ell_\Phi)}{\partial X_{zpd}} & \frac{\partial f(X,\ell_\Phi)}{\partial X_{N^j_{(j=1,nsat)}}} \end{bmatrix}$$

$$with: \frac{\partial f}{\partial X_x} = \frac{x - Xs}{\rho}, \quad \frac{\partial f}{\partial X_y} = \frac{y - Ys}{\rho}, \quad \frac{\partial f}{\partial X_z} = \frac{z - Zs}{\rho},$$

$$\frac{\partial f}{\partial X_{dt}} = C, \quad \frac{\partial f}{\partial X_{zpd}} = M, \quad \frac{\partial f}{\partial X_{N^j_{(j=1,nsat)}}} = 0 \quad or \quad 1$$

$$X = \begin{bmatrix} x \\ y \\ z \\ dt \\ zpd \\ N^j_{(j=1,nsat)} \end{bmatrix}.$$

The least squares solution with *a-priori* weighted constraints (P_x) to the parameters is given by:

$$\delta = -(P_{X^0} + A^T P_\ell A)^{-1} A^T P_\ell W, \quad (5)$$

so that the estimated parameters are

$$\hat{X} = X^0 + \delta,$$

with covariance matrix

$$C_{\hat{X}} = P_{\hat{X}}^{-1} = (P_{X^0} + A^T P_\ell A)^{-1}. \quad (6)$$

Adjustment Procedure

The adjustment procedure developed is effectively a sequential filter that adapts to varying user dynamics. The implementation considers the variations in the states of the parameters between observation epochs and uses appropriate stochastic processes to update their variances. The current model involves four types of parameters: station position (*x, y, z*), receiver clock (*dt*), troposphere zenith path delay (*zpd*) and carrier-phase ambiguities (*N*). The station position may be constant or change over time depending on the user dynamics. These dynamics could vary from tens of meters per second in the case of a land vehicle to a few kilometers per second for a low earth orbiter (LEO). The receiver clock will drift according to the quality of its oscillator, e.g. several centimeters/second in the case of an internal quartz clock with frequency stability of about 10^{-10}. Comparatively, the zenith path delay will vary in time by a relatively small amount, in the order of a few centimeters/hour. Finally, the non-integer carrier-phase ambiguities (*N*) will remain constant as long as the carrier phases are free of cycle-slips, a condition that requires close monitoring. (Note that only for double differenced data *dt* is practically eliminated and the carrier-phase ambiguities *(N)* become integers).

Using subscript *i* to denote a specific time epoch, we see that without observations between epochs, initial parameter estimates at epoch *i* are equal to the ones obtained at epoch *i-1*:

$$X_i^0 = \hat{X}_{i-1}. \quad (7)$$

To propagate the covariance information from epoch *i-1* to *i*, during an interval Δt, $C_{\hat{x}_{i-1}}$ has to be updated to include process noise represented by the covariance matrix $C\varepsilon_{\Delta t}$:

$$P_{X_i^0} = [C_{\hat{x}_{i-1}} + C\varepsilon_{\Delta t}]^{-1} \quad (8)$$

where

$$C\varepsilon_{\Delta t} = \begin{bmatrix} C\varepsilon(x)_{\Delta t} & 0 & 0 & 0 & 0 & 0 \\ 0 & C\varepsilon(y)_{\Delta t} & 0 & 0 & 0 & 0 \\ 0 & 0 & C\varepsilon(z)_{\Delta t} & 0 & 0 & 0 \\ 0 & 0 & 0 & C\varepsilon(dt)_{\Delta t} & 0 & 0 \\ 0 & 0 & 0 & 0 & C\varepsilon(zpd)_{\Delta t} & 0 \\ 0 & 0 & 0 & 0 & 0 & C\varepsilon(N^j_{(j=1,nsat)})_{\Delta t} \end{bmatrix}.$$

Process noise can be adjusted according to user dynamics, receiver clock behavior and atmospheric activity. In all instances $C\varepsilon(N^j_{(j=1,nsat)})_{\Delta t} = 0$ since the carrier-phase ambiguities remain constant over time.

In static mode, the user position is also constant and consequently $C\varepsilon(x)_{\Delta t} = C\varepsilon(y)_{\Delta t} = C\varepsilon(z)_{\Delta t} = 0$. In kinematic mode, it is increased as a function of user dynamics. The receiver clock process noise can vary as a function of frequency stability but is usually set to white noise with a large $C\varepsilon(dt)_{\Delta t}$ value to accommodate the unpredictable occurrence of clock resets. A random walk process noise of 5 mm/√hour is assigned to the zenith path delay $C\varepsilon(zpd)_{\Delta t}$.

Precise Point Positioning Correction Models

Developers of GPS software are generally well aware of corrections they must apply to pseudorange or carrier-phase observations to eliminate effects such as special and general relativity, Sagnac delay, satellite clock offsets, atmospheric delays, etc. (e.g. ION, 1980). All these effects are quite large, exceeding several meters, and must be considered even for pseudorange positioning at the meter precision level. When attempting to combine satellite positions and clocks precise to a few centimeters with ionospheric-free carrier phase observations (with millimeter resolution), it is important to account for some effects that may not have been considered in pseudorange or precise differential phase processing modes.

The following sections look at additional correction terms that are significant for carrier phase point positioning. They have been grouped under *Satellite Attitude Effects*, *Site Displacements Effects* and *Compatibility Considerations*. A number of the corrections listed below require the Moon or the Sun positions which can be obtained from readily available planetary ephemerides files, or more conveniently from simple formulas (as implemented here) since a relative precision of about 1/1000 is sufficient for corrections at the mm precision level. Note that for centimeter level differential positioning and baselines of less than 100 km, the correction terms discussed below can be safely neglected.

Satellite Attitude Effects

Satellite Antenna offsets

The requirement for satellite based corrections originates from the separation between the GPS satellite center of mass and the phase center of its antenna. Because the force models used for satellite orbit modeling refer to its center of mass, the IGS GPS precise satellite coordinates and clock products also refer to the satellite center of mass, unlike the orbits broadcast in the GPS navigation message that refer to satellite antenna phase center. However, the measurements are made to the antenna phase center, thus one must know satellite phase center offsets and monitor the orientation of the offset vector in space as the satellite orbits the Earth. The phase centers for most satellites are offset both in the body z coordinate direction (towards the Earth) and in the body x coordinate direction which is on the plane containing the Sun (see Figure 2).

Figure 2: **IGS Conventional Antenna Phase Center in Satellite Fixed Reference Frame (in meters)**

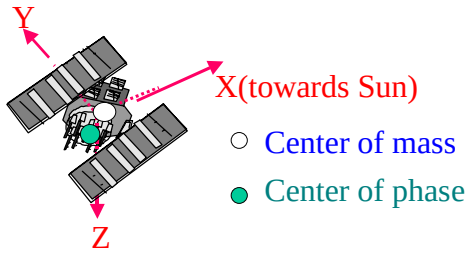

Antenna phase center offsets
in satellite fixed reference frame (meters)

	X	Y	Z
Block II/IIA:	0.279	0.000	1.023
Block IIR :	0.000	0.000	0.000

Phase Wind-Up Correction

GPS satellites transmit right circularly polarized (RCP) radio waves and therefore, the observed carrier-phase depends on the mutual orientation of the satellite and receiver antennas. A rotation of either receiver

or satellite antenna around its bore axis will change the carrier-phase up to one cycle (one wavelength), which corresponds to one complete revolution of the antenna. This effect is called "phase wind-up" (Wu et al., 1993). A receiver antenna, unless mobile, does not rotate and it is oriented towards a reference direction (usually north). However, satellite antennas undergo slow rotations as their solar panels are being oriented towards the Sun and the station-satellite geometry changes. Besides, during eclipsing seasons, satellites are also subjected to rapid rotations, so called "noon" and "midnight turns", to reorient their solar panels towards the Sun. This can represent antenna rotations of up to one revolution within less than half an hour. During such noon or midnight turns, phase data needs to be corrected for this effect or simply edited out.

The phase wind-up correction has been generally neglected even in the most precise differential positioning software, as it is quite negligible for double difference positioning on baselines/networks spanning up to a few hundred kilometers. Although, it has been shown that it can reach up to 4 cm for a baseline of 4000 km (Wu et al., 1993). However, this effect is quite significant for undifferenced point positioning when fixing IGS satellite clocks since it can reach up to one half of the wavelength. Since about 1994, most of the IGS Analysis Centers (and therefore the combined IGS orbit/clock products) apply this phase wind up correction. Neglecting it and fixing IGS orbits/clocks will result in position and clock errors at the dm level. For receiver antenna rotations (e.g. during kinematic positioning/navigation) phase wind-up is fully absorbed into station clock solutions (or eliminated by double differencing).

The phase wind-up correction can be evaluated from dot (·) and vector (×) products according to (Wu at al., 1993) as follows:

$$\Delta\phi = sign(\zeta)\ \cos^{-1}(\vec{D}'\cdot\vec{D}\,/\left|\vec{D}'\right\|\vec{D}\right|), \tag{9}$$

where $\zeta = \hat{k}\cdot(\vec{D}'\times\vec{D})$, $\hat{k}$ is the satellite to receiver unit vector and $\vec{D}', \vec{D}$ are the effective dipole vectors of the satellite and receiver computed from the current satellite body coordinate unit vectors ($\hat{x}', \hat{y}', \hat{z}'$) and the local receiver unit vectors ($\hat{x}, \hat{y}, \hat{z}$):

$$\vec{D}' = \hat{x}' - \hat{k}(\hat{k}\cdot\hat{x}') - \hat{k}\times\hat{y}',$$

$$\vec{D} = \hat{x} - \hat{k}(\hat{k}\cdot\hat{x}) + \hat{k}\times\hat{y}\ .$$

Continuity between consecutive phase observation segments must be ensured by adding full cycle terms of $\pm 2\pi$ to the correction (9).

Site Displacements Effects

In a global sense, a station undergoes real or apparent periodic movements reaching a few dm that are not included in the corresponding ITRF position. Consequently, if one is to obtain a precise station coordinate solution consistent with the current ITRF conventions, the above station movements must be modeled by adding the site displacement correction terms listed below to the conventional ITRF coordinates. Effects with magnitude of less than 1 centimeter such as atmospheric and snow build-up loading have not been considered in the following.

Solid Earth Tides

The "solid" Earth is in fact pliable enough to respond to the same gravitational forces that generate the ocean tides. The periodic vertical and horizontal site displacements caused by tides are represented by spherical harmonics of degree and order (*n m*) characterized by the Love number h_{nm} and the Shida number l_{nm}. The effective values of these numbers weakly depend on station latitude and tidal frequency (Wahr, 1981) and need to be taken into account when an accuracy of 1 mm is desired in determining station positions (see e.g. IERS Conventions (IERS, 1996)). However, for 5 mm precision, only the second degree tides, supplemented with a height correction term are necessary.

For the site displacement vector in Cartesian coordinates $\Delta\vec{r}^{\,T} = \left|\Delta x, \Delta y, \Delta z\right|$ (IERS, 1989):

$$\Delta\vec{r} = \sum_{j=2}^{3} \frac{GM_j}{GM} \frac{r^4}{R_j^3} \left\{ \left[3l_2 \left(\hat{R}_j \cdot \hat{r} \right) \right] \hat{R}_j + \left[3 \left(\frac{h_2}{2} - l_2 \right) \left(\hat{R}_j \cdot \hat{r} \right)^2 - \frac{h_2}{2} \right] \hat{r} \right\} +$$
$$\left[-0.025m \cdot \sin\phi \cdot \cos\phi \cdot \sin\left(\theta_g + \lambda \right) \right] \cdot \hat{r}, \qquad (10)$$

where GM, GM_j are the gravitational parameters of the Earth, the Moon ($j=2$) and the Sun ($j=3$); r, Rj are geocentric state vectors of the station, the Moon and the Sun with the corresponding unit vectors $\hat{r}$ and $\hat{R}_j$, respectively; l_2 and h_2 are the nominal second degree Love and Shida dimensionless numbers (0.609, 0.085); ϕ, λ are the site latitude and longitude (positive east) and θ_g is Greenwich Mean Sidereal Time. The tidal correction (10) can reach about 30 cm in the radial and 5 cm in the horizontal direction. It consists of a latitude dependent permanent displacement and a periodic part with predominantly semi diurnal and diurnal periods of changing amplitudes. The periodic part is largely averaged out for static positioning over a 24-hour period. However, the permanent part, which can reach up to 12 cm in mid latitudes (along the radial direction) remains in such a 24h average position. The permanent tidal distortion, according to the ITRF convention (IERS, 1996) has to be used as well. In other words, the complete correction (10), which includes both the permanent and periodical tidal displacements, must be applied to be consistent with the ITRF convention. Even when averaging over long periods, neglecting the correction (10) in point positioning would result in systematic position errors of up to 12.5 and 5 cm in the radial and north directions, respectively. Note that for differential positioning over short baseline (<100km), both stations have almost identical tidal displacements so that the relative positions over short baselines will be largely unaffected by the solid Earth tides. If the tidal displacements in the north, east and vertical directions are required, they can be readily obtained by multiplying (10) by the respective unit vectors.

Ocean Loading

Ocean loading is similar to solid Earth tides as it is dominated by diurnal and semi diurnal periods, but it results from the load of the ocean tides. While ocean loading is almost an order of magnitude smaller than solid Earth tides, it is more localized and by convention it does not have a permanent part. For single epoch positioning at the 5 cm precision level, or mm static positioning over 24h period and/or for stations that are far from the oceans, ocean loading can be safely neglected. On the other hand, for cm precise kinematic point positioning or precise static positioning along coastal regions over intervals significantly shorter than 24h, this effect has to be taken into account. Note that when the tropospheric zpd or clock solutions are required, the ocean load effects also have to be taken into account even for a 24h static point positioning processing, unless the station is far (> 1000 km) from the nearest coast line. Otherwise, the ocean load effects will map into the tropospheric zpd/clock solutions (Dragert, 2000), which may be significant particularly for the coastal stations. The ocean load effects can be modeled in each principal direction by the following correction term (IERS, 1996):

$$\Delta c = \sum_j f_j A_{cj} \cos(\omega_j t + \chi_j + u_j - \Phi_{cj}), \qquad (11)$$

where f_j and u_j depend on the longitude of lunar node (at 1-3 mm precision f_j =1 and u_j =0); the summation of j represents the 11 tidal waves designated as M_2, S_2, N_2, K_2, K_1, O_1, P_1, Q_1, M_f, M_m and $S_{sa.}$; ω_j and χ_j are the angular velocity and the astronomical arguments at time $t=0h$, corresponding to the tidal wave component j. The arguments χ_j can be readily evaluated by a FORTRAN routine *ARG* available from the IERS Convention ftp site: *ftp://maia.usno.navy.mil/conventions/chapter7/arg.f* .

The station specific amplitudes A_{cj} and phases Φ_{cj} for the radial, south (positive) and west (positive) directions are computed by convolution of Green functions utilizing the latest global ocean tide models as well as refined coastline database (e.g. Scherneck, 1991; Pagiatakis, 1992; Agnew, 1996). A table of the amplitudes A_{cj} and phases Φ_{cj} for most ITRF stations, computed by Scherneck (1993), is also available from the above ftp URL (*ftp://maia.usno.navy.mil/conventions/chapter7/olls25.bld*). Alternatively, software for evaluation of A_{cj} and Φ_{cj} at any site is available from Pagiatakis (1992). Typically, the M_2 amplitudes are the largest and do not exceed 5 cm in the radial and 2 cm in the horizontal directions for coastal stations. For

cm accuracy it is also necessary to augment the global tidal model with local ocean tides digitized, for example, from the local tidal charts. Future ITRF convention will likely also require a model for the geocenter variation (at a cm level), which is also of tidal origin. Consequently the station specific amplitude A_{cj} and phases Φ_{cj} would then include the geocenter (tidal) variation. In fact the IERS tabulation at the above ftp site already includes the tidal geocenter variation. One consequence of this new convention/approach is that for cm station position precision, the ocean load effect corrections must be included at all stations, even for those far from the ocean.

Earth Rotation Parameters (ERP)

The Earth Rotation Parameters (i.e. Pole position *Xp*, *Yp* and *UT1-UTC*), along with the conventions for sidereal time, precession and nutation facilitate accurate transformations between terrestrial and inertial reference frames that are required in global GPS analysis (see e.g. IERS, 1996). Then, the resulting orbits in the terrestrial conventional reference frame (ITRF), much like the IGS orbit products, imply, quite precisely, the underlying ERP. Consequently, IGS users who fix or heavily constrain the IGS orbits and work directly in ITRF need not worry about ERP. However, when using software formulated in an inertial frame, the ERP corresponding to the fixed orbits are required.

For point positioning processing formulated within the terrestrial frame, with the IGS orbits held fixed, the so called sub-daily ERP model, which is also dominated by diurnal and sub-diurnal periods of ocean tide origin, is still required to attain sub cm positioning precision. This results from the IERS convention for ERP, i.e. the IERS/IGS ERP series as well as ITRF positions do not include the sub-daily ERP variations, which can reach up to 3 cm at the surface of the earth. However, the IGS orbits imply the complete ERP, i.e. the conventional ERP plus the sub-daily ERP model. In order to be consistent, in particular for precise static positioning over intervals much shorter than 24 h, this sub-daily effect needs to be taken into account. Note that much like the ocean tide loading, the sub-daily ERP are averaged out to nearly zero over a 24h period.

This effect can be modeled, like all the tidal displacements, as apparent corrections (Δx, Δy, Δz) to the conventional (ITRF) station coordinates (x, y, z), evaluated from the instantaneous sub-daily ERP corrections (δXp, δYp, $\delta UT1$), i.e.

$$\Delta x = + y \cdot \delta UT1 + z \cdot \delta Yp \,, \tag{12}$$
$$\Delta y = - x \cdot \delta UT1 - z \cdot \delta Xp, \tag{13}$$
$$\Delta z = - x \cdot \delta Yp + y \cdot \delta Xp, \tag{14}$$

where each of the sub-daily ERP component corrections (δXp, δYp, $\delta UT1$) is obtained from the following approximation form, e.g. for the *Xp* pole component:

$$\delta Xp = \sum_{j=1}^{8} F_j \sin \xi j + G_j \cos \xi_j \,, \tag{15}$$

where ξj is the astronomical argument at the current epoch for the tidal wave component j of the eight diurnal tidal waves considered (M_2, S_2, N_2, K_2, K_1, O_1, P_1, Q_1), augmented with $n \cdot \pi/2$ ($n = 0, 1$ or -1) and F_j and G_j are the tidal wave coefficients derived from the latest global ocean tide models for each of the three ERP components. The above (conventional) FORTRAN routine, evaluating the sub-daily ERP corrections can also be obtained at the (IERS, 1996) ftp site: *ftp://maia.usno.navy.mil/conventions/chapter8/ray.f* .

Compatibility considerations

Positioning and GPS analyses that constrain or fix any external solutions/products need to apply consistent orbit/clock weighting, models and conventions. This is in particular true for precise point positioning and clock solutions/products. However, even for cm differential positioning, consistency with the IGS global solutions needs to be considered. This includes issues such as the respective version of ITRF, the IGS

ERP, the IGS orbit and station solutions used, the station logs (antenna offsets) and the adopted antenna calibration table (*IGS_01.pcv*) available at the IGS Central Bureau (http://igscb.jpl.nasa.gov).

The GPS System already has some well developed conventions, e.g. that only the periodic special relativity correction

$$\Delta T_{rel} = -2\vec{X}s \cdot \vec{V}s / c^2 \qquad (16)$$

is to be applied by all GPS users (ION, 1980). Here $\vec{X}s, \vec{V}s$ are the satellite position and velocity vectors and *c* is the speed of light. The same convention has also been adopted by IGS, i.e. all the IGS satellite clock solutions are consistent with this convention.

By an agreed convention, there are no group delay calibration corrections applied for the station and satellite (L2-L1) biases in all the IGS AC analyses, thus no such calibrations are to be applied when the IGS clock products are held fixed or constrained in dual frequency point positioning. Furthermore, a specific set of pseudorange observations consistent with the IGS clock products needs to be used even for point positioning utilizing phase observations, otherwise the clock solutions are significantly affected. This is a result of significant satellite dependent differences between L1 C/A ($P_{C/A}$) and P (P_1) code pseudoranges which can reach up to 2 ns (60 cm). IGS has been using the following conventional pseudorange observation set, which needs to be enforced when using the IGS orbit/clock products (*IGS Mail #2744*):

Up to April 02, 2000 (GPS Week 1056): $\boldsymbol{P_{C/A}}$ and $\boldsymbol{P'_2 = P_{C/A} + (P_2 - P_1)}$
After April 02, 2000 (GPS Week 1056): $\boldsymbol{P_1}$ and $\boldsymbol{P_2}$

Note that in case of C/A and P–code carrier phase observations there is no such problem and no need for any such convention. The GPS system specifications states the difference between the two types of phase observation on L1 is the same for all satellites and it is equal to a constant fraction of the L1 wavelength. This difference is fully absorbed into an insignificant offset of the station clock solutions. For more information on this convention and how to form the above pseudorange observation set for receivers, which do not give all the necessary observation types, see *IGS Mail #2744* available from the IGS CB Archives: *http://igscb.jpl.nasa.gov/mail/igsmail/2000/*.

Precise Point Positioning (PPP) Evaluation

All the above correction models except for ocean & atmospheric loading and sub-daily ERP effects were implemented, including satellite/clock weighting, in a program that runs on a personal computer. To evaluate our PPP implementation, daily sessions of dual frequency code and carrier observations from globally distributed IGS stations were processed for GPS week 1039 (December 5-11, 1999). Observations at 30 seconds interval were used to facilitate cycle slip detection. Station positions, clock offsets and troposphere zenith path delays as well as satellite ambiguity parameters were estimated at 15 minute intervals (corresponding to the epochs of available precise orbits and clocks in the IGS and AC orbit/clock products).

This section shows the parameter convergence of the PPP solution and evaluates the quality of the positions, tropospheric zpd's and station clocks obtained.

PPP Solution Convergence

PPP convergence as a function of time depends on initial parameter variances and the synergy of GPS pseudorange and carrier phase observations. At the initial epoch, because of unknown carrier-phase ambiguities, the solution relies entirely on the pseudorange observations and the quality of the position reflects GPS receiver code resolution and the multipath environment at the tracking station. As time passes and phase observations are added to the solution, the ionospheric free ambiguities and station position

components (in static mode) converge to constant values while the troposheric zpd and receiver clock parameters vary as a function of their assigned process noise. Figure 3 shows a daily plot of position and tropospheric parameter updates at 15-minute intervals. For this particular site, initial station coordinates differ from the known values by as much as 50 cm. Considering the latitude, longitude and height differences (*ΔLAT,ΔLON,ΔHGT*) as a function of time, we notice that centimeter convergence is reached after processing 8-12 epochs or 2-3 hours of observations. With high-rate satellite clocks at 30-second interval, this convergence time can be further reduced to less than 30 minutes.

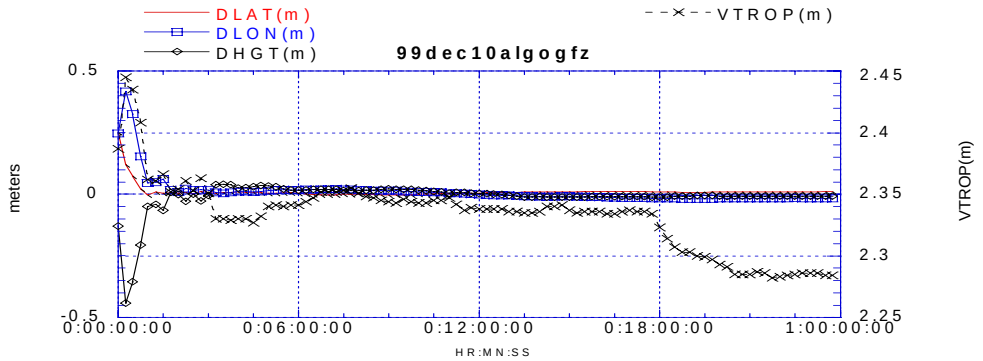

Figure 3. Precise Point Positioning Solution Convergence, December 10, 1999

PPP Station Coordinates Precision Evaluation

Data for each day of GPS week 1039 (December 5-11, 1999) was processed using up to 40 globally distributed GPS stations with tracking data of acceptable quality and continuity. The subset was selected from the 51 stations used by IGS for ITRF97 realization (Ferland, 2000). ITRF97 position estimates were used for comparison because they are very precise (sub-centimeter) . Daily differences in x, y and z were computed using Final orbit/clock files from 3 IGS Analysis Centers (EMR, GFZ and JPL) and the IGS Rapid and Final combined orbit/clock products (IGR, IGS). Figure 4 shows differences between the position estimates and the ITRF97 values for the 40 stations processed on December 11, 1999. Results obtained using EMR (Figure 4a) and IGS Final orbits (Figure 4b) were selected to illustrate that differences of several centimeters are still present in positions estimated using the orbits from certain AC's. It is also apparent that these coordinate differences are globally consistent for a specific day, that they correspond to "apparent geocenter offsets" and that they are greatly reduced through the IGS combination process.

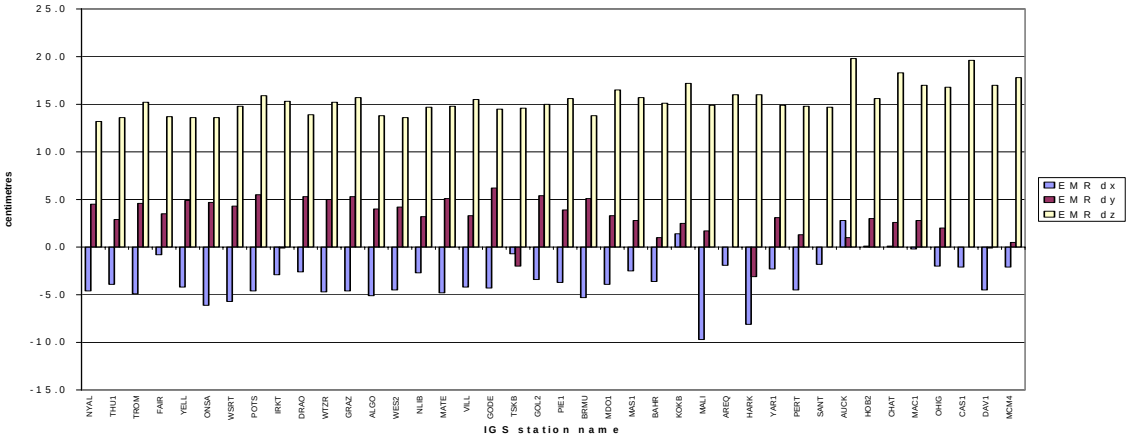

Figure 4a. Precise Point Positioning with EMR Final Orbits/Clocks -ITRF Position Differences (cm), December 11, 1999

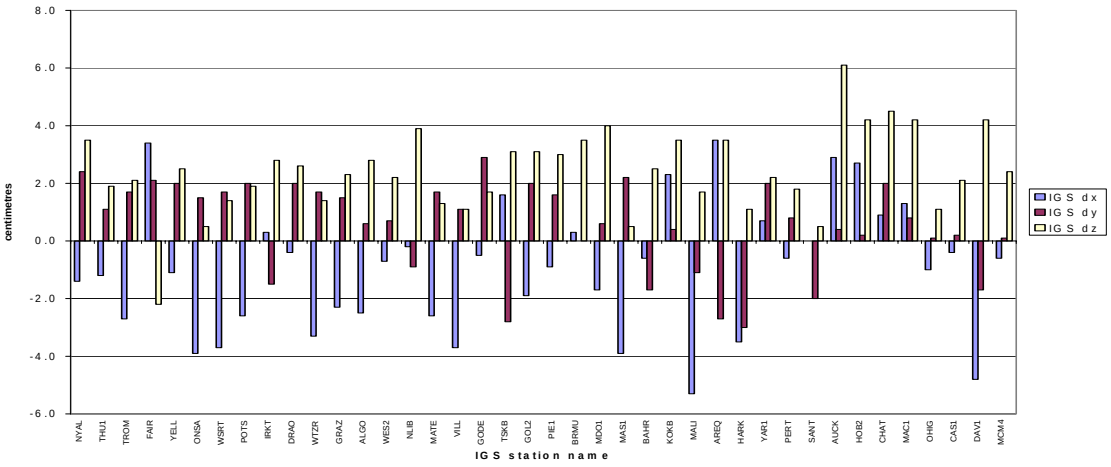

Figure 4b. Precise Point Positioning with IGS Final Orbits/Clocks -ITRF Position Differences (cm) , December 11, 1999

Table 1 gives average Cartesian coordinate differences and standard deviations for all stations and days of GPS week 1039. For all seven days, average differences are consistent at the centimeter level for all analysis centers except EMR, for which Δz daily bias varies by as much as 20 cm during this particular week. Nevertheless, in terms of precision, we see fairly stable daily standard deviations about the mean for all AC's over the entire week. It is interesting to note that the IGS Rapid product (IGR) is of comparable quality to the IGS Final and the best AC Final orbit/clock products.

Table 1. Daily Average Differences and Standard Deviations, GPS Week 1039

Average Δx, Δy, Δz (cm)																	
		EMR			GFZ			IGR			IGS			JPL			
Date	#Stn	Δx	Δy	Δz	Δx	Δy	Δz	Δx	Δy	Δz	Δx	Δy	Δz	Δx	Δy	Δz	
05-Dec-99	34	**1.7**	**2.4**	**10.0**	**-0.5**	**0.3**	**0.8**	**0.2**	**-0.9**	**1.1**	**0.1**	**0.5**	**2.0**	**-1.3**	**-0.6**	**4.1**	
06-Dec-99	32	**1.3**	**-0.1**	**-4.1**	**0.1**	**0.1**	**0.9**	**0.0**	**0.0**	**0.9**	**0.0**	**0.0**	**0.9**	**-0.8**	**-0.8**	**4.7**	
07-Dec-99	35	**1.6**	**2.7**	**7.1**	**-0.4**	**0.0**	**1.0**	**-0.4**	**0.1**	**0.7**	**-0.3**	**0.4**	**1.9**	**-1.0**	**-1.4**	**4.7**	
08-Dec-99	38	**-1.2**	**-0.1**	**3.8**	**-0.2**	**0.1**	**1.2**	**0.2**	**0.1**	**0.8**	**-0.1**	**-0.1**	**2.0**	**-1.5**	**-0.9**	**4.4**	
09-Dec-99	39	**-2.0**	**0.2**	**10.8**	**0.1**	**0.1**	**1.0**	**0.1**	**0.1**	**1.2**	**-0.1**	**-0.1**	**2.6**	**-1.1**	**-0.9**	**4.7**	
10-Dec-99	39	**1.4**	**0.7**	**2.7**	**0.0**	**-0.1**	**1.2**	**0.1**	**-0.2**	**1.1**	**0.2**	**0.3**	**1.8**	**-1.0**	**-1.2**	**4.9**	
11-Dec-99	40	**-3.3**	**2.8**	**15.4**	**0.0**	**0.1**	**1.3**	**0.2**	**-0.1**	**1.0**	**-1.0**	**0.6**	**2.4**	**-1.4**	**-0.7**	**4.5**	
Standard Deviation (about the mean in cm)																	
		EMR			GFZ			IGR			IGS			JPL			
Date	#Stn	σx	σy	σz	σx	σy	σz	σx	σy	σz	σx	σy	σz	σx	σy	σz	
05-Dec-99	34	**1.5**	**2.3**	**1.7**	**1.7**	**2.0**	**1.3**	**1.9**	**1.8**	**1.5**	**1.5**	**2.1**	**1.4**	**1.9**	**2.3**	**1.4**	
06-Dec-99	32	**2.3**	**2.2**	**1.6**	**2.1**	**1.9**	**1.2**	**2.3**	**2.1**	**1.2**	**1.9**	**2.0**	**1.2**	**2.1**	**2.3**	**1.3**	
07-Dec-99	35	**2.4**	**2.5**	**1.6**	**2.3**	**2.2**	**1.3**	**2.2**	**1.9**	**1.6**	**1.9**	**2.0**	**1.4**	**2.6**	**2.8**	**1.8**	
08-Dec-99	38	**2.3**	**2.9**	**1.8**	**1.8**	**1.7**	**1.4**	**1.8**	**1.9**	**1.6**	**1.7**	**1.9**	**1.4**	**1.9**	**2.1**	**1.6**	
09-Dec-99	39	**2.1**	**2.1**	**1.3**	**2.4**	**1.7**	**1.3**	**1.7**	**1.8**	**1.5**	**2.4**	**1.5**	**1.4**	**2.5**	**2.1**	**1.8**	
10-Dec-99	39	**1.8**	**2.3**	**1.7**	**1.9**	**1.6**	**1.5**	**1.7**	**2.0**	**1.8**	**1.9**	**1.8**	**1.6**	**1.9**	**2.1**	**1.8**	
11-Dec-99	40	**2.4**	**2.2**	**1.6**	**2.1**	**1.7**	**1.3**	**2.7**	**2.0**	**1.4**	**2.2**	**1.6**	**1.4**	**2.1**	**2.1**	**1.2**	

In Table 2, the daily average "apparent geocenter offsets" were removed from all the station Cartesian coordinate differences before transforming them into ellipsoidal. We now see that daily average ellipsoidal

coordinate differences are below 2 centimeters for all centers. One should also note the negative height bias of about 1 cm seen for all AC and IGS orbit/clock products. This bias is likely from PPP software origin and is currently being investigated. In terms of precision, we obtain fairly consistent standard deviations about the mean for all AC's over the entire week. As expected, the horizontal components are approximately two times more precise than the vertical.

Table 2. Daily Average Differences and Standard Deviations, GPS Week 1039

Average Δϕ, Δλ, Δh (cm)

		EMR			GFZ			IGR			IGS			JPL		
Date	#Stn	Δϕ	Δλ	Δh	Δϕ	Δλ	Δh	Δϕ	Δλ	Δh	Δϕ	Δλ	Δh	Δϕ	Δλ	Δh
05-Dec-99	34	**0.4**	**0.2**	**-1.5**	**0.0**	**-0.1**	**-1.3**	**0.2**	**-0.1**	**-0.6**	**0.1**	**-0.1**	**-1.3**	**0.3**	**0.0**	**-0.7**
06-Dec-99	32	**0.9**	**0.5**	**-1.5**	**0.3**	**0.0**	**-1.3**	**0.4**	**1.2**	**-1.1**	**0.4**	**0.1**	**-0.9**	**0.5**	**0.6**	**-0.8**
07-Dec-99	35	**1.0**	**0.2**	**-1.6**	**0.2**	**0.0**	**-1.1**	**0.3**	**0.5**	**-1.0**	**0.4**	**-0.1**	**-1.1**	**0.4**	**0.8**	**-1.3**
08-Dec-99	38	**0.5**	**1.1**	**-1.6**	**0.1**	**0.2**	**-0.9**	**0.2**	**0.4**	**-0.9**	**0.4**	**0.2**	**-1.1**	**0.3**	**0.7**	**-1.2**
09-Dec-99	39	**0.7**	**0.1**	**-1.9**	**0.3**	**0.0**	**-1.6**	**0.1**	**0.5**	**-1.1**	**0.4**	**0.0**	**-1.5**	**0.3**	**0.1**	**-1.9**
10-Dec-99	39	**0.5**	**0.6**	**-1.5**	**0.1**	**0.4**	**-1.3**	**0.2**	**1.1**	**-0.7**	**0.4**	**0.2**	**-1.1**	**0.4**	**0.1**	**-1.4**
11-Dec-99	40	**0.3**	**0.5**	**-2.0**	**0.0**	**0.7**	**-1.6**	**0.3**	**1.2**	**-1.3**	**0.5**	**0.3**	**-1.2**	**0.5**	**0.3**	**-1.6**

Standard Deviation (about the mean in cm)

		EMR			GFZ			IGR			IGS			JPL		
Date	#Stn	σϕ	σλ	σh	σϕ	σλ	σh	σϕ	σλ	σh	σϕ	σλ	σh	σϕ	σλ	σh
05-Dec-99	34	**1.0**	**1.4**	**2.2**	**1.1**	**1.3**	**2.0**	**1.3**	**1.3**	**2.4**	**1.1**	**1.4**	**1.9**	**1.4**	**1.7**	**2.3**
06-Dec-99	32	**1.1**	**1.8**	**2.2**	**1.2**	**1.5**	**2.0**	**1.3**	**1.6**	**1.9**	**1.1**	**1.6**	**2.0**	**1.2**	**1.8**	**2.3**
07-Dec-99	35	**0.8**	**1.8**	**2.7**	**1.2**	**1.5**	**2.5**	**1.1**	**1.6**	**2.5**	**1.1**	**1.4**	**2.2**	**1.2**	**2.0**	**3.1**
08-Dec-99	38	**1.2**	**1.8**	**2.8**	**1.1**	**1.4**	**2.0**	**1.1**	**1.4**	**2.2**	**1.1**	**1.3**	**2.1**	**1.2**	**1.5**	**2.2**
09-Dec-99	39	**1.0**	**1.2**	**1.9**	**1.1**	**1.3**	**2.2**	**1.1**	**1.3**	**2.0**	**1.1**	**1.2**	**2.2**	**1.0**	**1.6**	**2.6**
10-Dec-99	39	**1.1**	**1.7**	**2.1**	**1.0**	**1.5**	**1.8**	**1.1**	**1.5**	**2.2**	**1.0**	**1.5**	**2.2**	**1.0**	**1.4**	**2.3**
11-Dec-99	40	**1.2**	**1.5**	**2.2**	**1.2**	**1.2**	**1.8**	**1.4**	**1.5**	**2.4**	**1.1**	**1.3**	**2.2**	**1.4**	**1.2**	**1.9**

Tropospheric Zenith Path Delay Precision Evaluation

In addition to the station position and clock unknowns, the station tropospheric zenith path delays (zpds) are estimated at 15-minute intervals. As displayed in Figure 3, the station zpd estimates require a certain time to converge when the adjustment procedure is initiated using unconstrained parameters. One way of recovering the final zpd estimates (as well as station clocks) for all epochs is to smooth the parameters by a backward substitution with the final converged satellite ambiguity parameters held fixed. This approach, which approximates a rigorous backward filter (or back substitution in a batch least square processing), was implemented in the software to obtain nearly optimal station zpd (and station clock offset) time series based on all observation within the observation session (e.g. 24 h). Without such a back substitution scheme only the parameter solutions of the last epoch are optimal.

To evaluate the quality and consistency of our approach, the estimated zpds for the week 1039 using orbit products from different ACs were compared with the IGS combined tropospheric product (Gendt, 1998). IGS presently combines zpds at 2-hour intervals from contributions made by the seven ACs for up to 200 globally distributed GPS tracking stations. The IGS combined station zpds have been compared with estimates derived from other techniques and have proven to be quite precise (~7-8 mm) and accurate (Gendt, 1996).

Figure 5 shows a 7-day time series of zpds obtained from PPP for station YELL during GPS week 1039 using precise orbit products from EMR, GFZ, JPL, IGS and IGR. The IGS combined estimates (CMB) are also included. A general agreement between all time series is obvious.

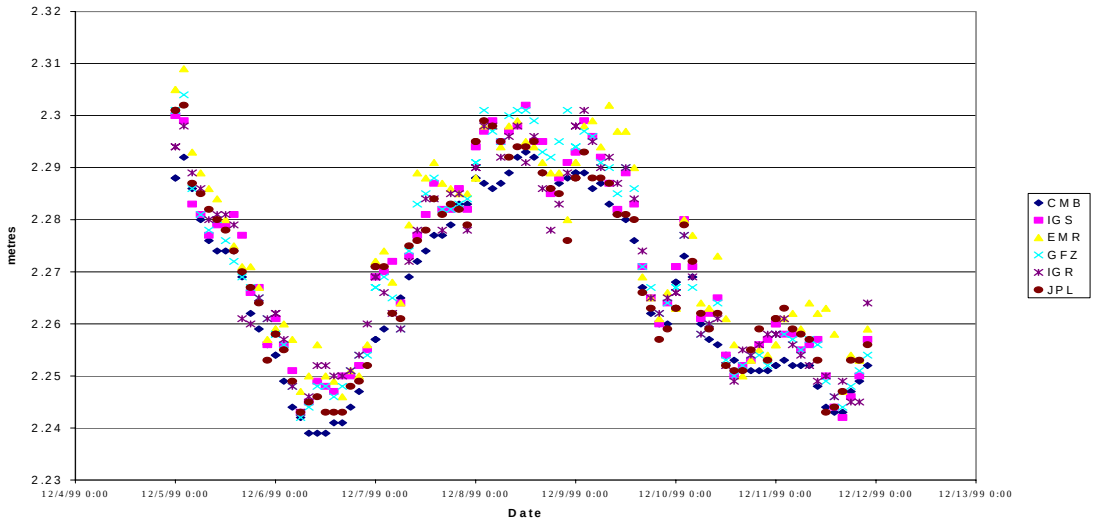

Figure 5. IGS Combined (CMB) Tropospheric zpd Solutions at Station YELL and PPP zpd Solutions (in m) Using IGS, IGR, EMR, GFZ and JPL orbit/clock Products.

To get a more global view of the quality of the zpd estimates, the daily means and standard deviations of differences with respect to the 2-hour IGS combined estimates are summarized in Table 3. These values were obtained from daily comparisons of approximately 30 IGS stations over the 7 days of the GPS week 1039. There are no apparent biases in the mean and standard deviations vary from 5 to 8 mm, corresponding to about 1 mm of integrated precipitable water (IPW).

Table 3. Tropospheric zpd Daily Average Differences and Standard Deviations with respect to IGS Combined zpd (in cm), GPS Week 1039

		EMR		GFZ		IGR		IGS		JPL	
Date	#Stn	Δzpd	σzpd	Δzpd	σzpd	Δzpd	σzpd	Δzpd	σzpd	Δzpd	σzpd
05-Dec-99	28	-0.3	0.7	-0.2	0.6	-0.5	0.7	-0.3	0.7	-0.2	0.6
06-Dec-99	28	-0.1	0.7	-0.2	0.6	-0.2	0.6	-0.1	0.6	0.0	0.8
07-Dec-99	31	-0.2	0.7	-0.1	0.7	-0.1	0.8	-0.1	0.7	-0.1	0.7
08-Dec-99	32	0.0	0.6	0.1	0.6	0.0	0.7	0.1	0.8	0.0	0.7
09-Dec-99	32	-0.3	0.6	-0.2	0.5	-0.2	0.7	-0.1	0.6	-0.5	0.6
10-Dec-99	33	0.0	0.7	0.1	0.7	0.3	0.7	0.1	0.7	0.1	0.6
11-Dec-99	32	-0.1	0.8	0.1	0.7	-0.2	0.9	0.0	0.8	-0.2	0.6

PPP Station Clock Precision Evaluation

Evaluating the quality of PPP estimated station clocks is somewhat complicated by the absence of an absolute standard for comparison and the fact that different reference clocks and alignment values are used by the ACs in the computation of their daily solutions. Therefore, the following evaluation is an internal comparison between the station clocks estimated with PPP and those produced by GFZ, JPL and EMR analysis centers (ACs).

Station Wetzell (WTZR) was selected for clock comparison since it is equipped with a Hydrogen MASER (HM) clock and processed by the 3 selected ACs for most days of GPS week 1039. The WTZR station clock solutions were extracted from daily station/satellite clock files submitted by EMR, GFZ and JPL in support of the IGS/BIPM precise timing pilot project (Ray, 1998). Table 4 shows the reference clock used by each AC in their daily clock computation. Note that the two reference stations (ALGO, NRC1) are also equipped with high quality HM clocks. Because of the requirement to set a station clock as reference in the AC network solutions, the WTZR station clock estimates will contain effects from both WTZR and the reference clocks.

For this test PPP used for input the 15-minute precise GPS satellite clocks stored in the AC final orbit product. Since the sp3 orbit/clock product files provide only orbit sigmas, no clock weighting was possible here. Table 4 gives the quality of the AC satellite clock estimates (converted to cm) as reported in the IGS final orbit combination summary (see igs10397.sum at IGS CB). Since the GPS satellite clocks implicitly contain the clock offset and drift of the AC selected reference clock, the resulting PPP estimated WTZR station clock offsets will also contain the effects of both WTZR and the reference clocks.

To remove the effect introduced by the different reference clocks offsets and drifts, and to check the solution quality, a daily linear regression was applied to the AC (EMR, GFZ, JPL) and PPP station clock estimates (EMR_SP3, GFZ_SP3, JPL_SP3) for WTZR. Since WTZR and all the clock reference stations are equipped with high quality HM clocks, 24-hour straight line RMS of fit of only a few cm should be expected. Table 4 gives the daily regression RMS of the WTZR 15-minute clock residuals obtained from the AC and PPP processing. These statistics show that the AC and PPP solutions of the WTZR clock have regression RMS at the 3-10 cm level (.1-.3 nanoseconds), which is consistent with the expected HM clock stability at or below 10^{-14}/100s. It is interesting to note that even though the IGS statistics for the quality of the AC satellite clock solutions (as reported in igs10397.sum) varies from 15 cm to 3 cm, the WTZR station clock obtained from PPP with the AC orbits/clock products is of comparable quality.

Table 4. Daily regression RMS of 15 minute clock residuals for station WTZR, GPS Week 1039

Date	EMR				GFZ				JPL			
	Ref Clock	SP3 Satellite Clock RMS (cm)	AC-WTZR Clock RMS (cm)	PPP WTZR Clock RMS (cm)	Ref Clock	SP3 Satellite Clock RMS (cm)	AC-WTZR Clock RMS (cm)	PPP WTZR Clock RMS (cm)	Ref Clock	SP3 Satellite Clock RMS (cm)	AC-WTZR Clock RMS (cm)	PPP WTZR Clock RMS (cm)
05-Dec-99	NRC1	15	4.0	4.0	ALGO	3	3.3	3.6	ALGO	12	4.0	6.2
06-Dec-99	ALGO	15	2.7	4.0	ALGO	6	2.9	3.1	ALGO	12		
07-Dec-99	ALGO	15	2.0	10.0	ALGO	3	3.3	3.3	ALGO	15		
08-Dec-99	NRC1	15	3.3	4.6	ALGO	3	2.0	3.6	NRC1	12	3.4	6.3
09-Dec-99	NRC1	15	5.1	4.6	ALGO	3	3.8	4.1	ALGO	12	3.1	2.7
10-Dec-99	ALGO	12	3.7	5.3	ALGO	3	4.0	5.1	ALGO	12	3.4	6.2
11-Dec-99	ALGO	18	3.2	3.9	ALGO	3	3.7	4.1	ALGO	15	2.9	2.4

Figure 6 shows the residuals for the 6 different solutions over the 7 days of week 1039. There is a systematic effect with peak-to-peak amplitude of ~20 cm. (.6 nanosecond) that corresponds well to what is expected from station GPS antenna cable temperature sensitivity (Larson, 2000). The AC and PPP solutions both contain the effects of such unmodeled temperature variations affecting the WTZR and the reference clocks (i.e. ALGO or NRC1). In this instance, no detectable temperature related clock variations are expected from ALGO or NRC1 since at both sites the antenna cables are shielded from the local environment.

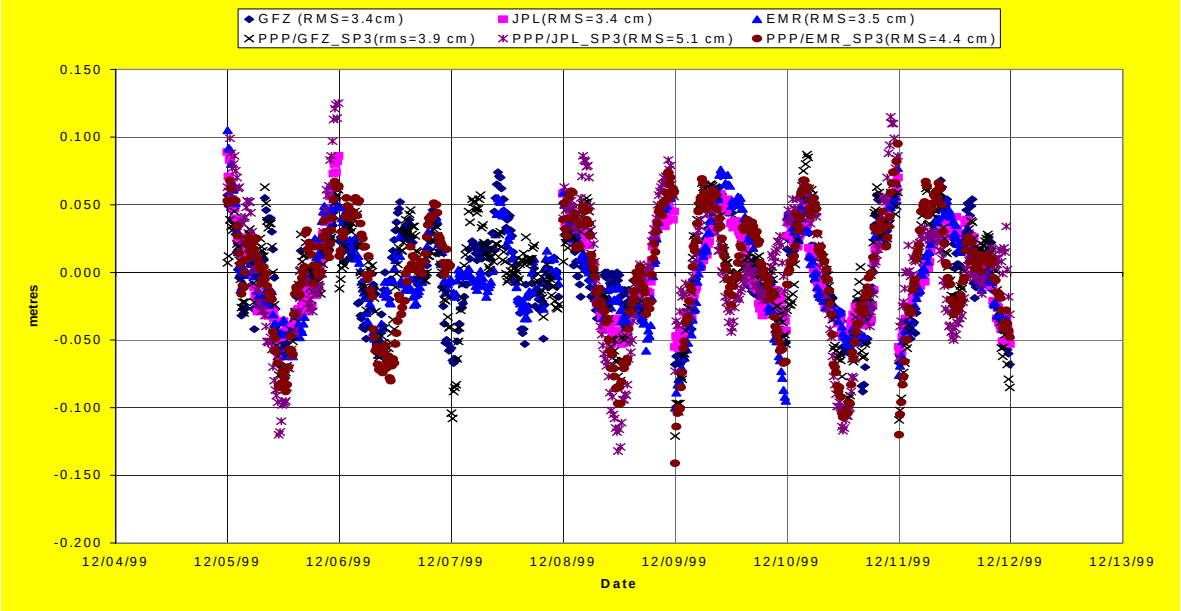

Figure 6. 24 h Linear Regression Clock Residuals from AC and PPP Estimates for Station WTZR Clock, GPS Week 1039

December 10 and 11 are the only two days of week 1039 where WTZR clock solutions are available from the three ACs with ALGO as a common reference. For those days, the linear regression residuals from the different solutions were differenced with respect to a particular AC in order to cancel out the common signal (e.g. temperature variation, HM clock instabilities) in order to assess the quality of the different solutions. Figure 7 shows the differenced WTZR clock residuals for 5 solutions with respect to GFZ. In comparison to the undifferenced clocks, there is a definite reduction in the RMS from the 3-6 cm to the 1.3-3 cm (40-100 picoseconds) level. Nevertheless, there are still some systematic effects noticeable in the time series (and Table 4), mainly in the PPP estimates which may be due to the fact that no PPP clock weighting was employed , however this requires further investigation.

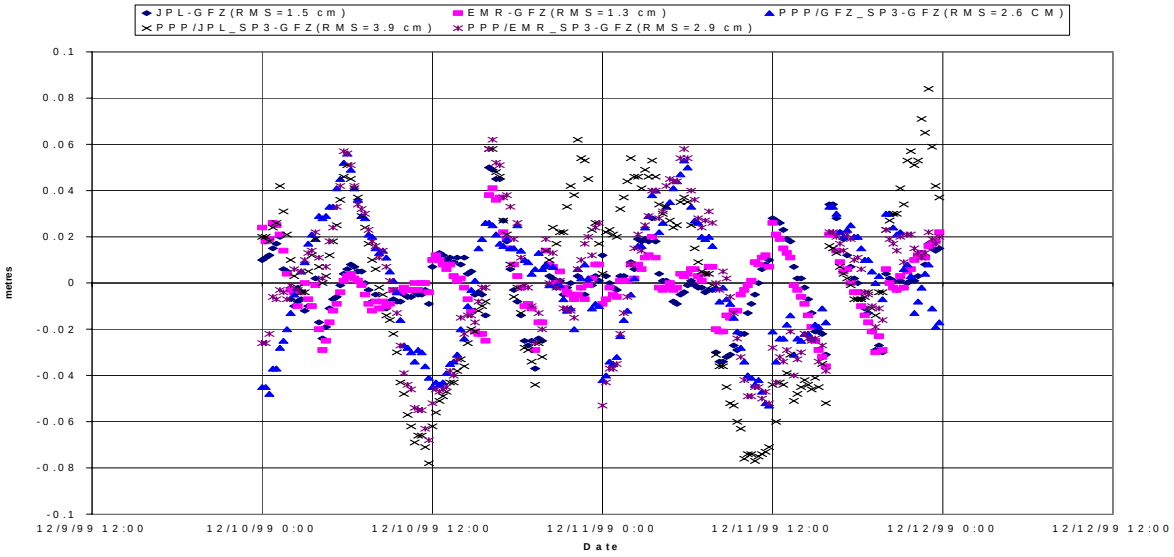

Figure 7. Differenced Clock Residuals from AC and PPP Estimates for Station WTZR, December 10-11, 1999

Conclusions

The observation equations, estimation technique and station/satellite models used for the implementation of GPS precise point positioning using IGS orbit/clock products were described. A post-processing approach that uses dual-frequency pseudorange and carrier-phase observations from a single GPS receiver and estimates station coordinates, tropospheric zenith path delays and clock parameters was developed and tested. Results show that global centimetre positioning precision can be realized, directly in ITRF, when using precise orbits/clock products from different IGS Analysis Centres (ACs) and the IGS combinations. The point positioning results also reveal the existence of apparent geocenter offsets between orbit products from different ACs. Furthermore, station tropospheric zenith path delays with centimetre precision and GPS receiver clock estimates precise to 0.1 nanoseconds can also be obtained using this technique. The single point positioning mode presented here forms an ideal interface to the IGS orbit/clock products and ITRF as it can be ported to a personal computer and executes with minimum user intervention. The approach is equally applicable to global kinematic positioning/navigation at the cm-dm precision level as is being demonstrated daily within IGS combination summary reports (see IGS Rapid and Final Combination Summary Reports at the IGS CB archives http://igscb.jpl.nasa.gov/mail/igsreport/igsreport.html)

Acknowledgements

The authors are grateful to the many individuals and organizations worldwide who contribute to the International GPS Service. IGS data and products are the result of an unprecedented voluntary, yet coordinated effort that continues to provide an invaluable service to the scientific community.

References

Agnew, D.C. (1996). SPOTL: Some programs for ocean-tide loading, SIO Ref. Ser. 96-8, Scripps Inst. of Oceanography, La Jolla, California.

Dragert, H., T.S. James, and A. Lambert (2000). Ocean Loading Corrections for Continuous GPS: A Case Study at the Canadian Coastal Site Holberg, Geophysical Research Letters, Vol. 27, No. 14, pp. 2045-2048, July 15, 2000.

Ferland, R. (1999). ITRF Coordinator report, 1999 IGS Annual Report, In press.

Héroux, P. and J. Kouba (1995). GPS Precise Point Positionning with a Difference, Paper presented at Geomatics ’95, Ottawa, Ontario, Canada, June 13-15.

Héroux, P., M. Caissy, and J. Gallace (1993). Canadian Active Control System Data Acquisition and Validation. Proceedings of the 1993 IGS (International GPS Service for Geodynamics) Workshop, University of Bern, pp. 49-58.

Gendt, G. (1998). IGS Combination of Tropospheric Estimates – Experience from Pilot Experiment, Proceedings of 1998 IGS Analysis Center Workshop, J.M. Dow, J. Kouba and T. Springer, Eds. IGS Central Bureau, Jet Propulsion Laboratory, Pasadena, CA, pp. 205-216.

Gendt, G. (1996). Comparison of IGS Troposphere Estimations, Proceedings of 1996 IGS Analysis Center Workshop, R.E. Neilan, P.A. Van Scoy and J.F. Zumberge, Eds. IGS Central Bureau, Jet Propulsion Laboratory, Pasadena, CA, pp. 151-164.

IERS (1989). IERS Standards (1989), IERS Technical Note 3, (ed. D.D. McCarthy)

IERS (1996). IERS Conventions (1996), IERS Technical Note 21, (ed. D.D. McCarthy)

ION (1980). Global Positioning System, Vol. I, Papers published in NAVIGATION,

ISBN:0-936406-00-3.

King, R. W., and Y. Bock (1999). Documentation of the GAMIT GPS Analysis Software (version 9.8), Unpublished, Massachusetts Institute of Technology, Cambridge, Massachusetts.

Kouba, J. (1998) IGS Analysis Activities (1998). IGS Annual Report, IGS Central Bureau, Jet Propulsion Laboratory, Pasadena, CA, pp. 13-17.

Kouba, J., Y. Mireault, G. Beutler, T. Springer, (1998). A Discussion of IGS Solutions and Their Impact on Geodetic and Geophysical Applications, GPS Solutions, Vol. 2, No. 2, pp. 3-15.

Larson, K.M., J. Levine, L.M. Nelson (2000). Assessment of GPS Carrier-Phase Stability for Time-Transfer Applications. IEEE Transactions on Ultrasonics, Ferroelectrics and Frequency Control, Vol. 47, No. 2, March 2000.

Lichten, S.M., Y.E. Bar-Sever, E.I. Bertiger, M. Heflin, K. Hurst, R.J. Muellerschoen, S.C. Wu, T.P. Yunck, and J. F. Zumberge (1995) GIPSY-OASIS II: A High precision GPS Data processing System and general orbit analysis tool, Technology 2006, NASA Technology Transfer Conference, Chicago, Il., Oct. 24-26.

Neilan, R.E., Zumberge, J.F., Beutler, G., & Kouba, J. (1997). The International GPS Service: A global resource for GPS applications and research. In Proc. ION-GPS-97 (pp. 883-889). The Institute of Navigation.

Pagiatakis,S.D. (1992). Program LOADSDP for the calculation of ocean load effects, Man. Geod., 17, 315-320.

Rothacher, M. and L. Mervart (1996). The Bernese GPS Software Version 4.0. Astronomical Institute, University of Berne, Berne, Switzerland.

Scherneck, H.G. (1991). A parameterized Solid Earth Tide Model and Ocean Tide Loading Effects for global geodetic baseline measurements, *Geophs. J. Int. 106*, pp. 677-694.

Scherneck, H.G. (1993). Ocean Tide loading: Propagation errors from ocean tide into loading coefficients, *Man. Geodetica, 18*, pp.59-71.

Wahr, J.M. (1981). The forced nutation of an elliptical, rotating, elastic, and oceanless Earth, Geophys. J. Roy. Astron. Soc., 64, pp. 705-727.

Wu, J.T., S,C. Wu, G.A. Hajj, W.I. Bertiger, and S.M. Lichten (1993). Effects of antenna orientation on GPS carrier phase, *Man. Geodetica 18*, pp. 91-98.

Zumberge, J.F. (1999). Automated GPS Data Analysis Service. GPS Solutions, Vol. 2, No, 3, pp.76-78.

Zumberge, J.F., Heflin, M.B., Jefferson, D.C., Watkins, M.M., & Webb, F.H. (1998). Precise point positioning for the efficient and robust analysis of GPS data from large networks. J. Geophys. Res., 102, 5005-5017.